Sphingosylphosphorylcholine induces proliferation of human adipose tissue-derived mesenchymal stem cells via activation of JNK

Eun Su Jeon,* Hae Young Song,* Mi Ra Kim,* Hyun Jung Moon,* Yong Chan Bae,† Jin Sup Jung,* and Jae Ho Kim[1,*,§]

Research Center for Ischemic Tissue Regeneration,* Department of Plastic Surgery, College of Medicine,† and Medical Research Institute,§ Pusan National University, Busan 602-739, Republic of Korea

Abstract Sphingosylphosphorylcholine (SPC) has been implicated in a variety of cellular responses, including proliferation and differentiation. In this study, we demonstrate that D-*erythro*-SPC, but not L-*threo*-SPC, stereoselectively stimulated the proliferation of human adipose tissue-derived mesenchymal stem cells (hADSCs), with a maximal increase at 5 μM, and increased the intracellular concentration of Ca^{2+} ($[Ca^{2+}]_i$) in hADSCs, which do not express known SPC receptors (i.e., OGR1, GPR4, G2A, and GPR12). The SPC-induced proliferation and increase in $[Ca^{2+}]_i$ were sensitive to pertussis toxin (PTX) and the phospholipase C (PLC) inhibitor U73122, suggesting that PTX-sensitive G proteins, Gi or Go, and PLC are involved in SPC-induced proliferation. In addition, SPC treatment induced the phosphorylation of c-Jun and extracellular signal-regulated kinase, and SPC-induced proliferation was completely prevented by pretreatment with the c-Jun N-terminal kinase (JNK)-specific inhibitor SP600125 but not with the MEK-specific inhibitor U0126. Furthermore, the SPC-induced proliferation and JNK activation were completely attenuated by overexpression of a dominant negative mutant of JNK2, and the SPC-induced activation of JNK was inhibited by pretreatment with PTX or U73122. Treatment of hADSCs with lysophosphatidic acid (LPA) receptor antagonist, Ki16425, had no impact on the SPC-induced increase in $[Ca^{2+}]_i$. However, SPC-induced proliferation was partially, but significantly, attenuated by pretreatment of the cells with Ki16425. These results indicate that SPC stimulates the proliferation of hADSCs through the Gi/Go-PLC-JNK pathway and that LPA receptors may be responsible in part for the SPC-induced proliferation.—Jeon, E. S., H. Y. Song, M. R. Kim, H. J. Moon, Y. C. Bae, J. S. Jung, and J. H. Kim. **Sphingosylphosphorylcholine induces proliferation of human adipose tissue-derived mesenchymal stem cells via activation of JNK. *J. Lipid Res.* 2006.** 47: **653–664.**

Supplementary key words c-Jun N-terminal kinase • phospholipase C • G proteins

Mesenchymal stem cells can be isolated from a variety of tissues, such as bone marrow, periosteum, trabecular bone, synovium, skeletal muscle, deciduous teeth, and adipose tissues (1). They possess self-renewal capacity, long-term viability, and differentiation potential toward the diverse cell types, such as adipogenic, osteogenic, chondrogenic, and myogenic lineages (1–6). Human adipose tissue-derived mesenchymal stem cells (hADSCs) have generated a great deal of interest because of their potential use in clinical applications and their stem cell-like properties. For clinical applications, however, it is necessary to maintain the self-renewal capacity and proliferation of hADSCs during ex vivo amplification of the cells. However, the molecular identities of extracellular agonists and intracellular signaling molecules, which regulate the self-renewal and proliferation of hADSCs, are largely unknown.

Lysophospholipids, such as sphingosine-1-phosphate (S1P), lysophosphatidic acid (LPA), lysophosphatidylcholine (LPC), and sphingosylphosphorylcholine (SPC), play a role in many areas of cellular physiology and pathophysiology (7–10). In particular, SPC takes part in several cellular responses, such as migration, wound healing, and differentiation (9, 11–13), and is known to stimulate DNA synthesis and proliferation in various cell types, including fibroblasts, endothelial cells, keratinocytes, and vascular smooth muscle cells, as a potent mitogen (9, 12, 14–16). In contrast to the above, SPC can also inhibit the growth

Abbreviations: BAPTA, 1,2-bis(*o*-aminophenoxy)ethane-*N,N,N,N*-tetraacetic acid; $[Ca^{2+}]_i$, intracellular concentration of Ca^{2+}; DN-JNK2, dominant negative mutant of JNK2; DN-MEK1, dominant negative mutant of MEK1; ERK, extracellular signal-regulated kinase; GFP, green fluorescent protein; GPCR, G protein-coupled receptor; GST, glutathione-*S*-transferase; HA, hemagglutinin; hADSC, human adipose tissue-derived mesenchymal stem cell; JNK, c-Jun N-terminal kinase; LPA, lysophosphatidic acid; LPC, lysophosphatidylcholine; MAP, mitogen-activated protein; MTT, 3-(4,5-dimethyl-2-thiozol)-2,5-diphenyl-2H-tetrazolium bromide; PTX, pertussis toxin; S1P, sphingosine-1-phosphate; SPC, sphingosylphosphorylcholine.

[1] To whom correspondence should be addressed.
e-mail: jhkimst@pusan.ac.kr

Manuscript received 24 June 2005 and in revised form 21 November 2005.

Published, JLR Papers in Press, December 7, 2005.
DOI 10.1194/jlr.M500508-JLR200

of various cell types, mostly that of tumor cells such as pancreatic, breast, and ovarian cancer cells and Jurkat T-cells (13, 17). We recently reported that SPC positively or negatively regulates the proliferation of hADSCs, depending on the concentrations of SPC exposed to hADSCs (18). However, the molecular mechanism involved in the SPC-induced regulation of proliferation is not clearly understood.

Mitogen-activated protein (MAP) kinases, including extracellular signal-regulated kinase (ERK), c-Jun N-terminal kinase (JNK), and p38, are the major signal transduction molecules regulated by growth factors, cytokines, and stress (19). Each member of the MAP kinases is activated by phosphorylation and subsequently translocates into the nucleus to promote diverse physiological responses (19). ERK is mainly activated by growth-promoting factors and participates in cell proliferation or survival, whereas JNK and p38 are mainly activated by stress signals and are known to induce apoptosis in many kinds of cells (19–21). Activated JNK phosphorylates serine-63 and serine-73 residues of c-Jun and increases the transcription activity of the AP-1 complex, which is responsible for the transcription of apoptosis-related genes (19–21). SPC has been reported to induce the phosphorylation of ERK in several cell types by activation of G protein-coupled receptors (GPCRs) (16, 22, 23). It has been demonstrated that ERK plays a key role in the SPC-stimulated proliferation of aortic smooth muscle cells (16) and the hypertrophic growth of rat neonatal cardiomyocytes (23). The SPC-induced activation of ERK and proliferation are mediated by pertussis toxin (PTX)-sensitive G proteins, such as Gi or Go (9, 13). Recently, we reported that treatment of hADSCs with concentrations of >10 μM SPC induced apoptotic cell death and that the SPC-induced activation of ERK was responsible for the cell death (18). However, treatment of hADSCs with concentrations of <5 μM SPC stimulated the proliferation of hADSCs. Therefore, it was not clear which subtypes of MAP kinases were involved in the SPC-induced proliferation of hADSCs. In this study, we demonstrate that SPC is a principal lysophospholipid to stimulate the proliferation of hADSCs and that JNK, but not ERK, plays a crucial role in the SPC-induced proliferation of hADSCs.

MATERIALS AND METHODS

Materials

Minimum essential medium α, phosphate-buffered saline, trypsin, and FBS were purchased from Invitrogen (Carlsbad, CA). SP600125 and 3-(4,5-dimethyl-2-thiozol)-2,5-diphenyl-2H-tetrazolium bromide (MTT) were from Calbiochem (La Jolla, CA). U0126, SB202190, and PTX were from Biomol (Plymouth Meeting, PA). S1P, LPC, and LPA were from Avanti Polar Lipids (Alabaster, AL). D-*erythro*-SPC and L-*threo*-SPC were from Matreya (Pleasant Gap, PA). Platelet-derived growth factor-BB (PDGF-BB) was purchased from R&D Systems, Inc. (Minneapolis, MN). The anti-phospho-ERK (Thr202/204), anti-phospho-p38 (Thr180/Tyr182), and anti-phospho-c-Jun (Ser63) antibodies were from Cell Signaling Technology (Beverly, MA). The anti-ERK antibody was from BD Biosciences (San Diego, CA). Peroxidase-labeled secondary antibodies and the enhanced chemiluminescence kit were purchased from Amersham Biosciences. Collagenase type I, Ki16425, and all other reagents were obtained from Sigma-Aldrich.

Cell culture

Subcutaneous adipose tissue was obtained from elective surgeries with the patients' consent, as approved by the Institutional Review Board, and hADSCs were isolated as reported previously (24). Briefly, adipose tissues were washed at least three times with sterile phosphate-buffered saline and treated with an equal volume of collagenase type I (1 g/l in Hank's balanced salt solution with 1% BSA) for 60 min at 37°C with intermittent shaking. The floating adipocytes were separated from the stromal-vascular fraction by centrifugation (300 *g* for 5 min). The pellet was resuspended in minimum essential medium α supplemented with 10% FBS, 100 U/ml penicillin, and 100 μg/ml streptomycin and plated in tissue culture dishes at 3,500 cells/cm^2. The primary hADSCs were cultured for 4–5 days until confluence and were defined as passage 0. The passage number of hADSCs used in the experiments was 3–10. The expression profiles of the hADSCs were highly similar to those of human bone marrow-derived mesenchymal stem cells, as observed using flow cytometric analysis and microarray analysis (25). The hADSCs were positive for CD29, CD44, CD90, and CD105, all of which have been reported to be marker proteins of mesenchymal stem cells. However, c-kit, CD34, and CD14, which are known as hematopoietic markers, were not expressed in the hADSCs.

Proliferation assay

Proliferation was determined by both direct counting with a hemocytometer using the trypan blue exclusion method and an indirect colorimetric MTT assay: MTT is metabolized by NAD-dependent dehydrogenase to form a colored reaction product, and the amount of dye formed directly correlates with the number of cells. For the determination of cell numbers, hADSCs were seeded on a 24-well culture plate at a density of 2×10^4 cells/well, cultured for 48 h in the growth medium, serum-starved for 24 h, and then treated with or without various reagents for the indicated times. For the MTT assay, the cells were washed twice with phosphate-buffered saline and incubated with 100 μl of MTT (0.5 mg/ml) for 2 h at 37°C. The formazan granules generated by the cells were dissolved in 100 μl of DMSO, and the absorbance of the solution at 562 nm was determined using a PowerWave$_x$ microplate spectrophotometer (Bio-Tek Instruments, Inc., Winooski, VT) after dilution to a linear range. For direct counting of cell number, the reagent-treated hADSCs were harvested by trypsinization, suspended in phosphate-buffered saline, and incubated with an equal amount of 0.1% trypan blue. The number of trypan blue-negative cells was counted using a hemocytometer.

Measurement of intracellular calcium concentration

Spatially averaged photometric [Ca^{2+}] measurements from single cells were performed with the fluorescent Ca^{2+} indicator fluo-4-AM (Molecular Probes, Inc., Eugene, OR). Thus, hADSCs were seeded in a 32 mm dish, loaded with 5 μM fluo-4-AM for 40 min at 37°C in buffer A (135 mM NaCl, 4 mM KCl, 1 mM $MgCl_2$, 2 mM $CaCl_2$, 10 mM glucose, and 20 mM HEPES, pH 7.3), and washed twice with Hanks' balanced salt solution without phenol red and Ca^{2+}. The fluo-4-AM-loaded cells were treated with the appropriate concentration of SPC. In some experiments, 0.2 mM EGTA was added in the Hanks' balanced salt solution without phenol red and Ca^{2+} to titrate out extracellular

Ca^{2+} during measurement of the intracellular concentration of Ca^{2+} ($[Ca^{2+}]_i$). A Leica TCS-SP2 laser scanning confocal microscope (Leica Microsystems) was used to visualize Ca^{2+}-mediated fluorescence in the cells. Fluo-4 was excited with the 488 nm line of an argon laser, and fluo-4 fluorescence was collected between 510 and 525 nm. Scanning was performed every 1 s for the indicated times after treatment with SPC, and the ratio of fluorescence intensity to initial fluorescence intensity was calculated at each point for quantitative measurement.

Western blotting

Confluent serum-starved hADSCs were treated under appropriate conditions, washed with ice-cold phosphate-buffered saline, and then lysed in lysis buffer (20 mM Tris-HCl, 1 mM EGTA, 1 mM EDTA, 10 mM NaCl, 0.1 mM phenylmethanesulfonyl fluoride, 1 mM Na_3VO_4, 30 mM sodium pyrophosphate, 25 mM β-glycerol phosphate, and 1% Triton X-100, pH 7.4). Lysates were resolved by SDS-PAGE and transferred onto a nitrocellulose membrane. After blocking with 5% nonfat milk, the membranes were immunoblotted with anti-phospho-ERK (Thr202/204), anti-phospho-p38 (Thr180/Tyr182), and anti-ERK at a dilution of 1:1,000. The bound primary antibodies were probed with horseradish peroxidase-conjugated secondary antibodies and visualized by the enhanced chemiluminescence Western blotting system.

JNK activity assay

JNK activity was measured by the glutathione-based pull-down method using a kit from Cell Signaling Technology (Beverly, MA) according to the manufacturer's directions. Briefly, cell extracts (0.2 mg of protein) were incubated with 1 μg of immobilized glutathione-*S*-transferase-c-Jun(1–79) fusion protein, centrifuged, washed, and incubated in kinase buffer (25 mM Tris-HCl, pH 7.5, 5 mM β-glycerophosphate, 2 mM dithiothreitol, 0.1 mM Na_3VO_4, 10 mM $MgCl_2$, and 10 μM ATP) for 30 min at 30°C. Phosphorylated substrate was detected by SDS-PAGE and immunoblotting using the phospho-specific c-Jun (Ser63) antibody (dilution, 1:1,000).

Overexpression of dominant negative mutants of JNK2 and MEK1

Recombinant adenoviruses expressing the green fluorescent protein (GFP) or coexpressing GFP and hemagglutinin (HA)-tagged dominant negative mutant of JNK2 (DN-JNK2) have been described (26). Subconfluent hADSCs were infected with adenoviruses bearing GFP or GFP plus HA-tagged DN-JNK2 at 100–150 plaque-forming units/cell for 1 h. After removing the adenovirus, cells were cultured for an additional 24 h in fresh growth medium. A dominant negative mutant of MEK1 (DN-MEK1) was overexpressed using a retrovirus system as described previously (27). pMSCVpuro retroviral vector (Clontech, Palo Alto, CA) containing DN-MEK1 was introduced into HEK293T cells (packaging cell line) with 1 μg of pVSV-G vector (Clontech) using the LipofectAMINE Plus reagents according to the instructions from the manufacturer. The next day, virus supernatant from these cells was added with 5 μg/ml Polybrene to hADSCs. After 24 h of incubation, the medium was replaced with fresh medium. The expression levels of DN-JNK2 and DN-MEK1 were determined by Western blotting with anti-HA antibody.

RT-PCR analysis

mRNA was isolated using a QIAshredder and an RNeasy kit (Qiagen, Hilden, Germany). mRNA, Moloney murine leukemia virus reverse transcriptase, and pd(N)6 primers (GIBCO BRL, Gaithersburg, MD) were used to obtain cDNA. The primers used for the RT-PCR analysis have been reported previously (28). The sequences of the primers used were as follows; LPA_1 receptor (349 bp product): sense, 5′-TCTTCTGGGCCATTTTCAAC-3′; antisense, 5′-TGCCTRAAGGTGGCGCTCAT-3′. LPA_2 receptor (798 bp product): sense, 5′-CCTACCTCTTCCTCATGTTC-3′; antisense, 5′-TAAAGGGTGGAGTCCATCAG-3′. LPA_3 receptor (382 bp product): sense, 5′-GGAATTGCCTCTGCAACATCT-3′; antisense, 5′-GAGTAGATGATGGGGTTCA-3′. GAPDH (246 bp product): sense, 5′-GATGACATCAAGAAGGTGGTGAA-3′, antisense, 5′-GTCTTACTCCTTGGAGGCCATGT-3′. We ran 30 PCR cycles of 94°C (denaturation, 1 min), 55°C (annealing, 1 min), and 72°C (extension, 1 min). PCR products were electrophoresed on a 2% agarose gel and visualized by ethidium bromide staining.

RESULTS

SPC induces the proliferation of human hADSCs

We measured the proliferation of hADSCs by the MTT assay method after treatment of the cells with the indicated concentrations of lysophospholipids for 48 h. As shown in **Fig. 1A**, treatment of hADSCs with D-*erythro*-SPC, a naturally occurring stereoisomer of SPC, stimulated proliferation at 50 nM and dose-dependently increased the proliferation with a maximal peak at 5 μM. However, concentrations of D-*erythro*-SPC of >10 μM caused apoptotic cell death, as demonstrated previously (18). Exposure of hADSCs to LPA and LPC also induced proliferation, with maximal stimulation at 2 and 5 μM, respectively. Nevertheless, the stimulatory effects of both LPA and LPC were less than that of D-*erythro*-SPC, and S1P had no effect on the proliferation of hADSCs. hADSCs exhibited fibroblast-like morphologies and slowly proliferated in the absence of exogenous SPC, whereas treatment of the cells with 5 μM D-*erythro*-SPC drastically increased the cell number in a time-dependent manner (Fig. 1B, C). The D-*erythro*-SPC-induced increase in cell numbers was comparable to the increase mediated by PDGF-BB, which is known as a potent mitogen in mesenchymal cell types (29), although the SPC- or PDGF-induced proliferation was less potent than the increase induced by 10% FBS (Fig. 1B, C). These results suggest that not only PDGF-BB but also SPC is a potent mitogen stimulating the proliferation of hADSCs in the absence of FBS.

SPC stereoselectively increases intracellular Ca^{2+} and stimulates the proliferation of hADSCs

Extracellular SPC has been shown to increase $[Ca^{2+}]_i$ in a variety of cell types (9, 13), and the D-*erythro*, but not the L-*threo* stereoisomer, of SPC increases $[Ca^{2+}]_i$ by binding to its cognate GPCRs (30). To explore whether SPC stereoselectively triggers the increase of $[Ca^{2+}]_i$ in hADSCs, we examined the effect of SPC on $[Ca^{2+}]_i$ in fluo-4-loaded hADSCs, as described in Materials and Methods. Treatment of hADSCs with 5 μM D-*erythro*-SPC rapidly increased $[Ca^{2+}]_i$ (**Fig. 2A**); however, treatment of hADSCs with 5 μM L-*threo*-SPC did not increase $[Ca^{2+}]_i$ (Fig. 2B). These results suggest that the D-*erythro* stereoisomer of SPC specifically increases $[Ca^{2+}]_i$, and that the

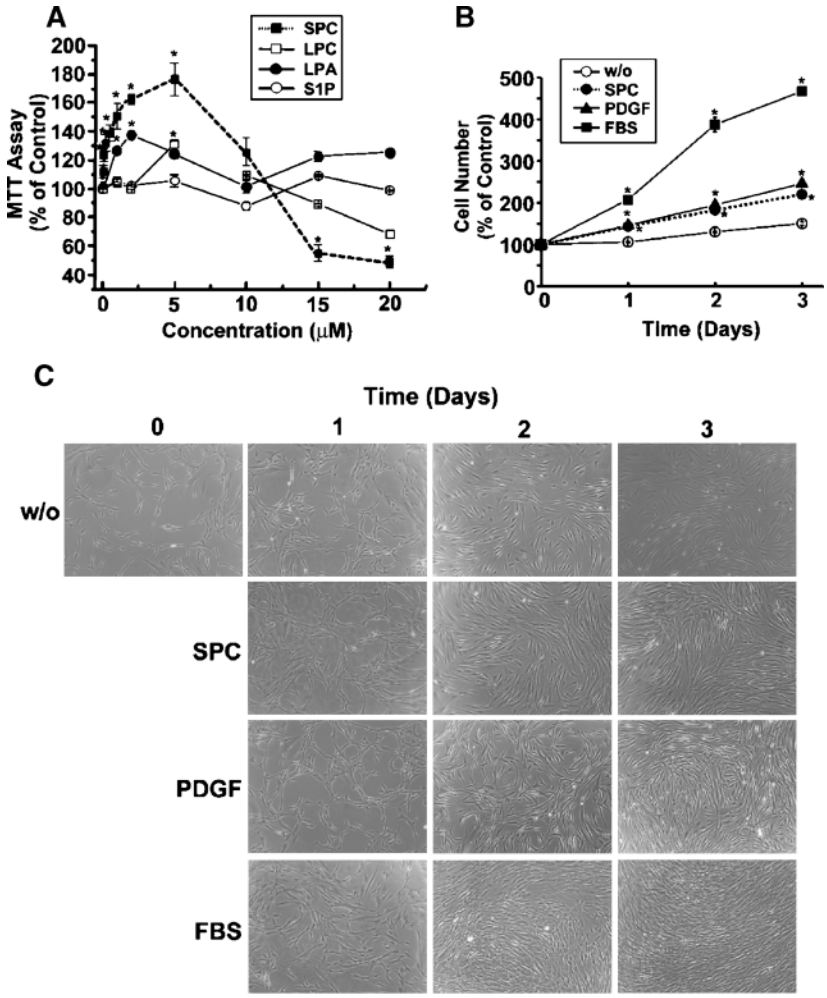

Fig. 1. Effects of lysophospholipids on the proliferation of human adipose tissue-derived mesenchymal stem cells (hADSCs). A: hADSCs were plated on 24-well culture plates at a density of 2×10^4 cells/well, cultured for 48 h in the growth medium, serum-starved for 24 h, and then treated with the indicated concentrations of lysophospholipids for 48 h. The cell numbers were determined by 3-(4,5-dimethyl-2-thiozol)-2,5-diphenyl-2H-tetrazolium bromide (MTT) assay as described in Materials and Methods. Results are expressed as percentages of vehicle-treated controls. B: Serum-starved hATSCs were treated with vehicle (w/o; 0.1% DMSO), 5 μM D-*erythro*-sphingosylphosphorylcholine (SPC), 25 ng/ml PDGF-BB, or 10% FBS for the indicated times. The cell numbers were measured using a hemocytometer, and results are shown as percentages of controls (0 h). Data are expressed as means ± SEM (n = 4) and are representative of three independent experiments. Student's *t*-test was used for paired values. * $P < 0.05$. C: Phase-contrast images of hADSCs treated under the conditions indicated were made with a digital camera equipped with inverted microscopy (Olympus IX70). Data are representative of three similar experiments.

SPC-induced increase of $[Ca^{2+}]_i$ may be mediated by the specific activation of SPC receptors. To assess whether the SPC-induced proliferation of hADSCs is specific to the stereoisomers of SPC, we examined the effect of D-*erythro* and L-*threo* stereoisomers on the proliferation of hADSCs. Consistent with the stereospecificity of the SPC-induced increase of $[Ca^{2+}]_i$, D-*erythro*-SPC, but not L-*threo*-SPC, specifically stimulated the proliferation of hADSCs (Fig. 2C).

SPC-induced increase of $[Ca^{2+}]_i$ is mediated by release of Ca^{2+} from intracellular stores

To further confirm the SPC-induced increase of $[Ca^{2+}]_i$, we determined the effects of 1,2-bis(*o*-aminophenoxy) ethane-*N,N,N,N*-tetraacetic acid (BAPTA)-AM, a chelating agent of intracellular Ca^{2+}, on the levels of $[Ca^{2+}]_i$. Pretreatment of hADSCs with BAPTA-AM completely abrogated the D-*erythro*-SPC-induced increase of $[Ca^{2+}]_i$ (Fig. 2D). To explore whether the D-*erythro*-SPC-induced increase of $[Ca^{2+}]_i$ was attributable to the influx of extracellular Ca^{2+}, we next examined the effect of D-*erythro*-SPC on $[Ca^{2+}]_i$ in the presence of EGTA, a chelating agent of extracellular Ca^{2+}. As shown in Fig. 2E, the SPC-induced increase of $[Ca^{2+}]_i$ was unaffected by the removal of extracellular Ca^{2+}. Therefore, these results indicate that the D-*erythro*-SPC-induced increase of $[Ca^{2+}]_i$ is not mediated by an influx of extracellular Ca^{2+} in hADSCs.

SPC-induced increase of $[Ca^{2+}]_i$ and proliferation are mediated by activation of Gi/Go and phospholipase C

It has been reported that the SPC-induced increase of $[Ca^{2+}]_i$ was mediated by PTX-sensitive G proteins, such as Gi or Go, in several cell types (9, 13). To assess whether the SPC-induced increase of $[Ca^{2+}]_i$ and proliferation was mediated by PTX-sensitive G proteins, we examined the effects of PTX on the $[Ca^{2+}]_i$ and cell numbers in hADSCs. As shown in **Fig. 3A**, pretreatment of hADSCs with 100 ng/ml PTX completely abolished the D-*erythro*-SPC-induced increase of $[Ca^{2+}]_i$. Because the SPC-induced increase of $[Ca^{2+}]_i$ was mediated by mobilizing Ca^{2+} from intracellular stores, but not by influx of extracellular Ca^{2+}, we next explored whether phospholipase C (PLC) was involved in the SPC-induced increase of $[Ca^{2+}]_i$. Pretreatment of hADSCs with U73122, a PLC inhibitor, completely prevented the SPC-induced increase of $[Ca^{2+}]_i$ (Fig. 3B). Consistent with these results, SPC-induced proliferation was completely prevented by pretreatment with either PTX or U73122 (Fig. 3C). These results suggest that Gi/Go- and PLC-dependent pathways are involved

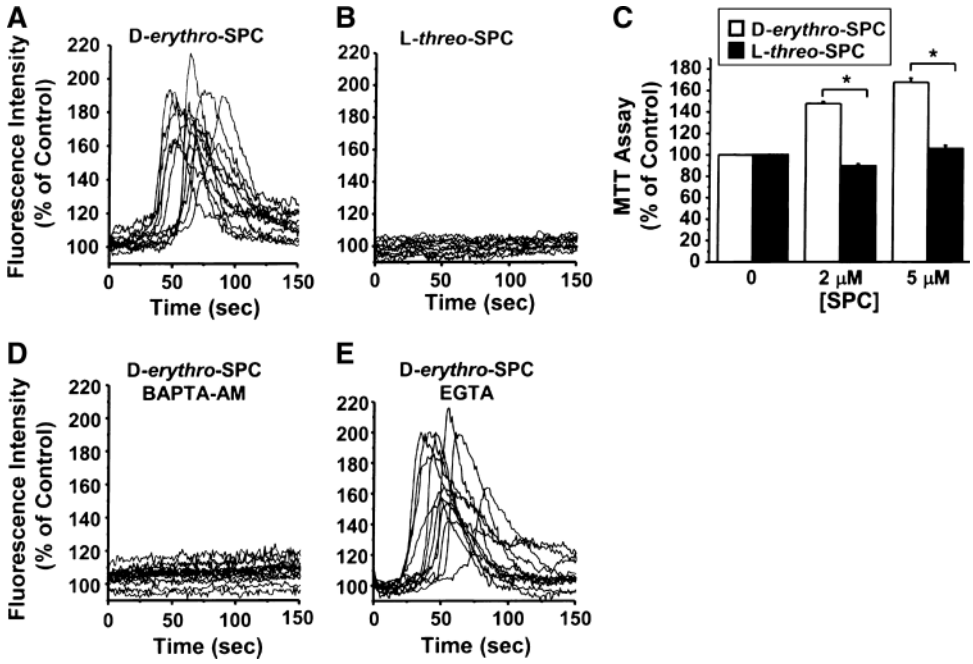

Fig. 2. Effects of SPC on the intracellular concentration of Ca^{2+} ($[Ca^{2+}]_i$) and the proliferation of hADSCs. A, B: Serum-starved hADSCs were loaded with 5 μM fluo-4-AM for 40 min at 37°C and exposed to 5 μM D-*erythro*-SPC (A) or 5 μM L-*threo*-SPC (B). Ca^{2+}-dependent fluorescence was measured every second for the indicated times, and fluorescence intensities of >12 different cells from time-lapse images were quantified over time. Representative data from three similar experiments are shown, and results are expressed as percentages of controls (0 s). C: Serum-starved hADSCs were exposed to the indicated concentrations of L-*threo*-SPC and D-*erythro*-SPC for 48 h. Proliferation was determined by the MTT assay. Results are expressed as percentages of controls (0 h). Data are shown as means ± SEM ($n = 4$) and are representative of three independent experiments. * $P < 0.05$ by Student's *t*-test. D, E: Serum-starved hADSCs were loaded with fluo-4-AM for 40 min at 37°C in the presence of 35 μM 1,2-bis(*o*-aminophenoxy)ethane-*N,N,N,N*-tetraacetic acid (BAPTA-AM; D) or 0.2 mM EGTA (E). The cells were then exposed to 5 μM D-*erythro*-SPC to measure Ca^{2+}-dependent fluorescence for the indicated times.

in the SPC-induced increase of $[Ca^{2+}]_i$ and proliferation in hADSCs.

JNK is involved in the SPC-induced proliferation of hADSCs

To explore whether SPC induces the activation of MAP kinases, we measured the effect of exogenous SPC on JNK activity and the phosphorylation of ERK and p38 MAP kinases. JNK activity was determined by measuring the JNK-dependent phosphorylation of c-Jun, as described in Materials and Methods. Phosphorylation of c-Jun occurred in response to treatment with 5 μM D-*erythro*-SPC for 10 min, and the SPC-induced phosphorylation of c-Jun at serine-63 was completely abolished by pretreatment with SP600125, a JNK-specific inhibitor, but not with either U0126 or SB202190 (**Fig. 4A**, **B**). These results suggest that the SPC-induced phosphorylation of c-Jun is dependent specifically on JNK activation. In addition, SPC treatment induced the phosphorylation of ERK, which could be completely prevented by pretreatment with U0126, a MEK-specific inhibitor, but not with SP600125 or SB202190 (Fig. 4C). Treatment of the cells with SPC did not induce the phosphorylation of p38, although phosphorylation of both p38 and JNK was highly stimulated by treatment with anisomycin, which is well known to stimulate JNK and p38 (31). These results indicate that SPC induces the activation of JNK and ERK in hADSCs and that SP600125 and U0126 specifically block the SPC-induced activation of JNK and ERK, respectively. To clarify whether MAP kinases are involved in SPC-induced proliferation, we examined the effect of MAP kinase inhibitors on the proliferation of hADSCs. As shown in Fig. 4D, pretreatment of the cells with SP600125 completely attenuated SPC-induced proliferation, whereas pretreatment with U0126 or SB202190 had little impact on SPC-induced proliferation, suggesting that JNK, but not ERK or p38, is primarily involved in SPC-induced proliferation.

DN-JNK2 blocks the SPC-induced proliferation of hADSCs

To further confirm the finding that JNK is involved in the SPC-induced proliferation of hADSCs, we next explored the effects of DN-JNK2 on the SPC-induced proliferation and phosphorylation of c-Jun. Adenoviral expression of DN-JNK2 has been reported to specifically block JNK-dependent signaling (26); therefore, HA-tagged DN-JNK2 and GFP were coexpressed in hADSCs by the adenovirus system. **Figure 5A** shows that infection of adenoviruses expressing GFP or coexpressing GFP and HA-tagged DN-JNK2 elicited the expression of GFP in most hADSCs, as judged by fluorescence microscopy. As shown in Fig. 5B,

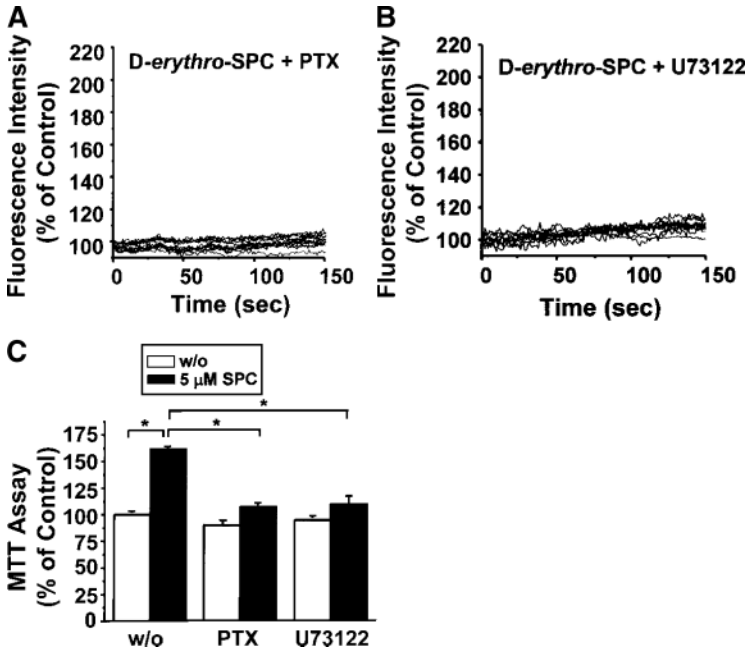

Fig. 3. Effects of pertussis toxin (PTX) or U73122 on the SPC-induced increase of $[Ca^{2+}]_i$ and proliferation. A: hADSCs were seeded onto 32 mm dishes and incubated with serum-free medium in the presence of 100 ng/ml PTX for 24 h. The cells were loaded with fluo-4-AM for 40 min at 37°C in the presence of 100 ng/ml PTX and exposed to 5 μM D-*erythro*-SPC. B: Serum-starved hADSCs were loaded with fluo-4-AM for 40 min at 37°C in the presence of 5 μM U73122 and then exposed to 5 μM D-*erythro*-SPC. Ca^{2+}-dependent fluorescence was measured every second for the indicated times after the addition of D-*erythro*-SPC, and fluorescence intensities of >12 different cells from time-lapse images were quantified over time. Representative data from three similar experiments are shown. C: To determine the effects of PTX-sensitive G proteins and PLC on proliferation, hADSCs were plated on 24-well culture plates and pretreated with 100 ng/ml PTX for 24 h or 5 μM U73122 for 15 min. The cells were then exposed to 5 μM D-*erythro*-SPC for 48 h. Cell number was determined by MTT assay. Results are expressed as percentages of controls (0 h). Data are shown as means ± SEM ($n = 4$) and are representative of three independent experiments. * $P < 0.05$ by Student's *t*-test.

the expression of HA-tagged DN-JNK2 was determined by Western blotting with anti-HA antibody. Next, to explore whether the DN-JNK2 blocked the SPC-induced phosphorylation of c-Jun, we measured the JNK activity in the hADSCs infected with HA-tagged DN-JNK2. In the GFP-expressing hADSCs, SPC treatment induced the phosphorylation of c-Jun. However, coexpression of GFP and HA-tagged DN-JNK2 completely attenuated the SPC-induced phosphorylation of c-Jun (Fig. 5C). These results led us to conclude that overexpression of DN-JNK2 can abrogate the SPC-induced activation of JNK in hADSCs.

To confirm the contention that JNK plays a crucial role in the SPC-induced proliferation of hADSCs, we next explored the effects of DN-JNK2 on SPC-induced proliferation. As shown in Fig. 5D, SPC increased the proliferation of hADSCs infected with adenovirus bearing GFP, used as a control. However, adenoviral overexpression of HA-tagged DN-JNK2 blocked SPC-induced proliferation, which was determined by MTT assay.

To further explore whether the MEK-ERK pathway is involved in SPC-induced proliferation, we examined the effects of DN-MEK1 on the SPC-induced proliferation and activation of ERK. As shown in Fig. 5E, overexpression of DN-MEK1 inhibited the SPC-induced phosphorylation of ERK. However, overexpression of DN-MEK1 could not attenuate the SPC-induced proliferation in hADSCs (Fig. 5F). Together, these results indicate that JNK, but not ERK, plays a pivotal role in SPC-induced proliferation.

SPC activates JNK through PTX-sensitive and PLC-dependent pathways

It has been reported that the SPC-induced activation of ERK is mediated by Gi/Go-dependent activation of PLC (9, 13, 16, 22). Because SPC-induced proliferation required the activation of Gi/Go, PLC, and JNK, we next explored whether the SPC-induced activation of JNK was dependent on Gi/Go and PLC. Pretreatment of hADSCs with either PTX or U73122 significantly attenuated the SPC-induced activation of JNK (**Fig. 6A**, **B**). These results suggest that the SPC-induced activation of JNK, which occurs through the Gi/Go-PLC pathway, plays an important role in the SPC-induced proliferation of hADSCs.

Partial involvement of LPA receptors in SPC-induced proliferation

Lysophospholipid-induced physiological responses occurred by the activation of PTX-sensitive G proteins, Gi or Go, in a variety of cell types (32–35). Recently, the Gi/Go-JNK pathway has been reported to play a role in the LPA-induced migration of glioma cells (32). In this study, we demonstrated that LPA as well as SPC stimulates the proliferation of hADSCs, although the stimulatory effects of LPA were less potent than those of SPC. Using RT-PCR analysis, we observed that three LPA receptors, LPA_1, LPA_2, and LPA_3, are expressed in hADSCs (**Fig. 7A**). Therefore, we sought to examine whether the SPC-induced proliferation is mediated by the activation of LPA receptors. To determine whether the LPA receptors mediate SPC-induced signal transduction, we examined the effects of Ki16425, an antagonist for LPA_1 and LPA_3 receptors, on the SPC-induced increase of $[Ca^{2+}]_i$. LPA treatment induced rapid and robust increases of $[Ca^{2+}]_i$ (Fig. 7B), and pretreatment of the cells with Ki16425 completely abolished the LPA-induced increase in $[Ca^{2+}]_i$ (Fig. 7C). In contrast, the SPC-induced increase in $[Ca^{2+}]_i$ was not affected by pretreatment of the cells with Ki16425 (Fig. 7D). These results suggest that LPA receptors are not involved in the SPC-induced increase in $[Ca^{2+}]_i$ and do not serve as SPC receptors. To explore whether the SPC-induced proliferation of hADSCs requires the activation of LPA receptors, we next examined the effects of Ki16425 on SPC-induced proliferation. As shown in Fig. 7E, treatment

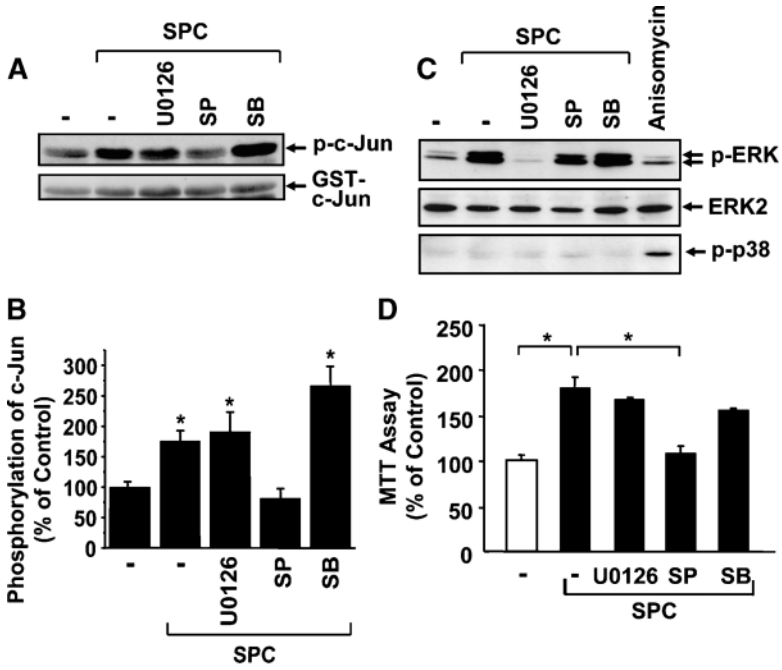

Fig. 4. Role of mitogen-activated protein (MAP) kinases in SPC-induced proliferation. A: Serum-starved hADSCs were pretreated with vehicle (solid line; 0.1% DMSO), 10 μM U0126, 10 μM SP600125 (SP), or 10 μM SB202190 (SB) for 15 min at 37°C and then exposed to 5 μM D-*erythro*-SPC for 10 min. An immobilized glutathione-*S*-transferase (GST)-c-Jun protein was used to pull down c-Jun N-terminal kinase (JNK) enzymes from cell lysates. Upon addition of kinase buffer and ATP, the phosphorylation of GST-c-Jun was probed by Western blotting using anti-phospho-c-Jun (Ser63) antibody (upper panel). The amounts of GST-c-Jun were determined by staining with Ponceau S solution (lower panel). Representative data of three independent experiments are shown. B: The densities of p-c-Jun and GST-c-Jun were quantified from three independent experiments, and the phosphorylation levels of c-Jun were normalized to the amounts of GST-c-Jun in the samples. The data are presented as percentages of controls (mock-treated cells) and expressed as means ± SEM of three independent experiments. C: Phosphorylation of extracellular signal-regulated kinase (ERK) and p38 was probed by Western blotting of the cell lysates with anti-phospho-ERK and anti-phospho-p38 antibodies, respectively, and the amounts of ERK were probed by anti-ERK antibody to confirm equal loading. Data are representative of three independent experiments. D: hADSCs were serum-starved for 24 h, pretreated with vehicle (solid line; 0.1% DMSO), 10 μM U0126, 10 μM SP600125 (SP), or 10 μM SB202190 (SB) for 15 min at 37°C, and then exposed to 5 μM D-*erythro*-SPC for 48 h. Proliferation was probed by the MTT assay. Results are expressed as percentages of vehicle-treated controls. Data are shown as means ± SEM ($n = 4$) and are representative of three independent experiments. * $P < 0.05$ by Student's *t*-test.

of hADSCs with LPA for 2 days increased cell numbers up to ~130% of control, and pretreatment of the cells almost completely blocked the LPA-induced proliferation. Interestingly, SPC-induced proliferation was significantly suppressed by pretreatment of the cells with Ki16425, suggesting that LPA_1 and/or LPA_3 partially mediates the proliferation induced by long-term treatment of the cells with SPC. Although Ki16425 treatment incompletely attenuates SPC-induced proliferation, these results suggest that activation of the LPA receptor plays a crucial role in the SPC-induced proliferation, but not in the SPC-stimulated increase in $[Ca^{2+}]_i$, in hADSCs.

DISCUSSION

In this study, we demonstrate that SPC dose-dependently increased the proliferation of hADSCs, with a maximal stimulation at 5 μM. The SPC-induced proliferation of hADSCs and increase of $[Ca^{2+}]_i$ were stereospecific to D-*erythro*-SPC but not to L-*threo*-SPC. In addition, pretreatment of hADSCs with PTX or U73122 completely prevented SPC-induced proliferation and the increase of $[Ca^{2+}]_i$. These results indicate that the SPC-induced increase in $[Ca^{2+}]_i$ and proliferation of hADSCs may require the Gi/Go-coupled receptor-dependent activation of PLC. Furthermore, we demonstrated that the Gi/Go-PLC-dependent activation of JNK is also required for the SPC-induced proliferation of hADSCs. A lot of different GPCRs were shown to activate JNK; however, the underlying mechanisms are still poorly understood (33, 36). It has been reported that $G\alpha_{i2}$ and $G\beta\gamma$ subunits released from $G\alpha\beta\gamma$ complexes upon stimulation of GPCRs are involved in the activation of JNK (33, 37) and that a variety of signaling enzymes, including PLC, PKC, Pyk2, focal adhesion kinases, and diverse GEFs for Rho family GTPases, are implicated in the G protein subunit-mediated activation of JNK (33, 36). These results support the

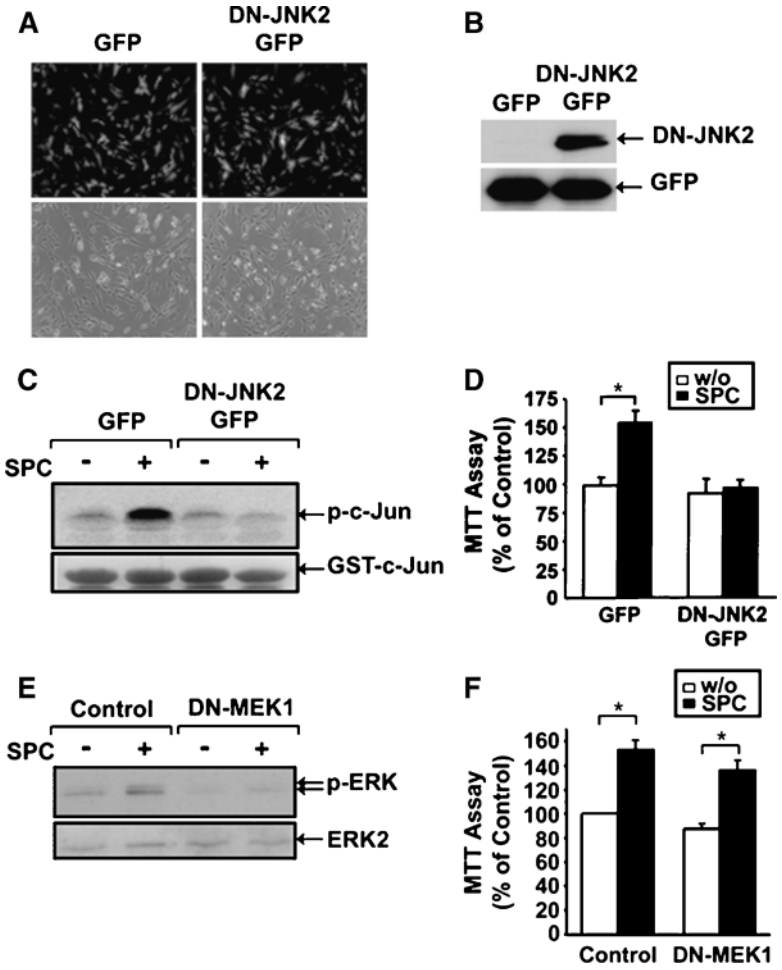

Fig. 5. Effect of a dominant negative mutant of JNK2 (DN-JNK2) on the SPC-induced proliferation of hADSCs. A: Subconfluent hADSCs were infected with adenovirus bearing green fluorescent protein (GFP) or GFP plus hemagglutinin (HA)-tagged DN-JNK2 for 1 h and cultured for an additional 24 h. The expression of GFP was determined with a fluorescence microscope (Olympus IX70) equipped with a digital camera. Excitation was delivered at 485 ± 11 nm, and emitted fluorescence was collected at 530 ± 15 nm (upper panels). Phase-contrast images are shown in the lower panels. B: Cell lysates of hADSCs infected with the adenoviruses were loaded onto SDS-polyacrylamide gels, and expression of HA-tagged DN-JNK2 and GFP was probed by Western blotting with anti-HA and anti-GFP antibodies, respectively. C: hADSCs were infected with adenovirus bearing GFP or GFP plus HA-tagged DN-JNK2 as indicated, serum-starved for 24 h, and then treated with vehicle (0.1% DMSO) or 5 μM D-*erythro*-SPC for 10 min. An immobilized GST-c-Jun protein was used to pull down JNK enzymes from cell lysates. Upon addition of kinase buffer and ATP, the phosphorylation of GST-c-Jun was probed by Western blotting using anti-phospho-c-Jun (Ser63) antibody (upper panel). The amounts of GST-c-Jun were determined by staining with Ponceau S solution (lower panel). D: To determine the effects of DN-JNK2 on SPC-induced proliferation, hADSCs were infected with adenovirus bearing GFP or GFP plus HA-tagged DN-JNK2 and then treated with vehicle (0.1% DMSO) or 5 μM D-*erythro*-SPC for 48 h as indicated. Proliferation was determined by the MTT assay, and results are expressed as percentages of vehicle-treated controls (GFP-expressed hADSCs). E: hADSCs were infected with retrovirus bearing a dominant negative mutant of MEK1 (DN-MEK1), serum-starved for 24 h, and then treated with vehicle (0.1% DMSO) or 5 μM D-*erythro*-SPC for 10 min. Phosphorylation of ERK was probed by Western blotting of the cell lysates with anti-phospho-ERK antibody, and the amounts of ERK were probed by anti-ERK antibody to confirm equal loading. F: To determine the effects of DN-MEK1 on SPC-induced proliferation, hADSCs were infected with the DN-MEK1 retrovirus and then treated with vehicle (0.1% DMSO) or 5 μM D-*erythro*-SPC for 48 h as indicated. Proliferation was determined by the MTT assay, and results are expressed as percentages of vehicle-treated controls. Data are shown as means ± SEM ($n = 4$) and are representative of three independent experiments. * $P < 0.05$.

present study, suggesting that $G\alpha_i$ and/or $G\beta\gamma$ play a crucial role in SPC-induced proliferation through the activation of PLC and JNK in hADSCs. Further studies concerning the molecular mechanism of the PLC-mediated activation of JNK would provide more detailed understanding of SPC-induced proliferation.

Several GPCRs, such as OGR1, GPR4, G2A, and GPR12, were recently identified as high-affinity receptors for SPC

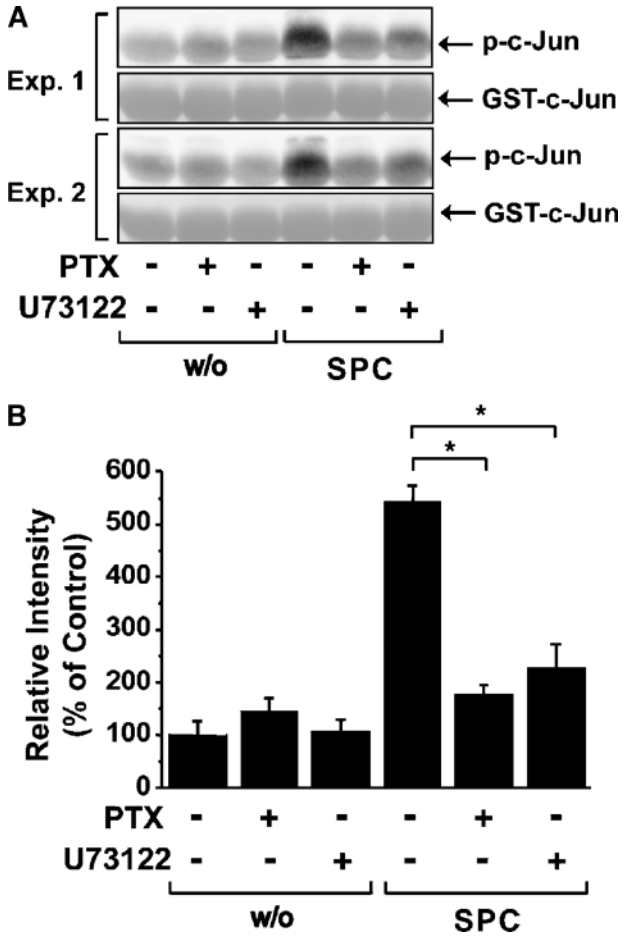

Fig. 6. Effects of PTX or U73122 on the SPC-induced activation of JNK. A: Serum-starved hADSCs were pretreated with 100 ng/ml PTX for 24 h or 5 μM U73122 for 15 min at 37°C and then exposed to 5 μM D-*erythro*-SPC for 10 min. An immobilized GST-c-Jun protein was used to pull down JNK enzymes from cell lysates. Upon addition of kinase buffer and ATP, the phosphorylation of GST-c-Jun was probed by Western blotting using anti-phospho-c-Jun (Ser63) antibody (upper panels). The amounts of GST-c-Jun were determined by staining with Ponceau S solution (lower panel). Representative data from three independent experiments in duplicate determinations are shown. B: The densities of p-c-Jun and GST-c-Jun were quantified from the representative data (A), and the phosphorylation levels of c-Jun were normalized to the amounts of GST-c-Jun in the samples. The data are presented as percentages of controls (mock-treated cells).

(9, 13). However, we observed that these SPC receptors were not expressed in hADSCs, when examined by RT-PCR (18). Furthermore, recent accumulating evidence demonstrates that OGR1, GPR4, and G2A are activated by proton but not by SPC (38–40). These results suggest that the SPC-induced proliferation and increase in $[Ca^{2+}]_i$ may not be dependent on these known SPC receptors. Several reports have provided evidence to indicate that S1P receptors act as low-affinity receptors for SPC (9, 13). However, in contrast to SPC-stimulated proliferation, we demonstrate here that S1P had no impact on the proliferation of hADSCs (Fig. 1A). We demonstrate that the inhibition of LPA_1 and LPA_3 by Ki16425 treatment significantly abrogated any LPA-induced increase in $[Ca^{2+}]_i$, in contrast to the lack of impact on the SPC-induced increase of $[Ca^{2+}]_i$. These results suggest that SPC-induced proliferation is partially mediated by the activation of LPA receptors (i.e., LPA_1 and/or LPA_3), whereas the LPA receptors are not likely to serve as SPC receptors (Fig. 7). A possible explanation for the implication of LPA receptors in SPC-induced proliferation is that treatment of hADSCs with SPC for 2 days may elicit the production of LPA, and the subsequent activation of LPA_1 or LPA_3 by the released LPA may play a role in the SPC-induced proliferation (**Fig. 8**).

To prove this possibility, it should be clarified whether LPA can be produced by SPC treatment, and the molecular mechanisms involved in the SPC-induced production of LPA need to be explored further, because diverse enzymes, including autotoxin, phospholipase A_2, and phospholipase D, have been implicated in LPA production (41, 42). In addition, the involvement of the Gi/Go-PLC-JNK pathway in the LPA receptor-mediated indirect pathway (Fig. 8) needs to be determined further. In spite of a crucial role of LPA receptors in SPC-induced proliferation, Ki16425 treatment could not completely prevent SPC-induced proliferation. These results suggest that SPC-induced proliferation may be mediated in part by the activation of unidentified SPC receptors (Fig. 8). Another possibility is that LPA_2 may be responsible for the Ki16425-independent proliferation of hADSCs in response to SPC treatment, because Ki16425 is an antagonist specific for LPA_1 and LPA_3. To clarify these contentions, it is necessary to confirm the involvement of the LPA receptors in SPC-induced proliferation by RNA interference technology.

SPC has been shown to induce the activation of ERK in a variety of cell types (13, 22). In this study, we demonstrate for the first time that not only ERK but also JNK was activated by SPC treatment and that JNK plays a major role in the SPC-induced proliferation of hADSCs. Pharmacological inhibition of JNK activation or overexpression of DN-JNK2 attenuated the SPC-induced proliferation of hADSCs, whereas inhibition of ERK had only a marginal effect on PDGF-induced proliferation. In contrast, we demonstrate that cell death caused by treatment of hADSCs with high concentrations of SPC could be completely prevented by inhibition of ERK but not by JNK inhibition (18). These results appear to be contradictory to previous findings that ERK and JNK play a key role in growth factor-induced proliferation and in stress-induced apoptosis, respectively (19), and that ERK is involved in SPC-induced proliferation in aortic smooth muscle cells (16). Nevertheless, recent accumulating evidence suggests that JNK plays a key role in cell survival and the proliferation of various cell types (20, 43). Inhibition of basal JNK activity by SP600125 or antisense oligonucleotides attenuated the proliferation of KB-3 human carcinoma cells (44), and SP600125 inhibited cyclin D1 expression and proliferation during liver regeneration (45). Furthermore, both overexpression of a dominant negative mutant of JNK and the pharmacological inhibition of JNK blocked the PDGF-induced proliferation of smooth muscle cells (46, 47). Consistent with these findings, we also

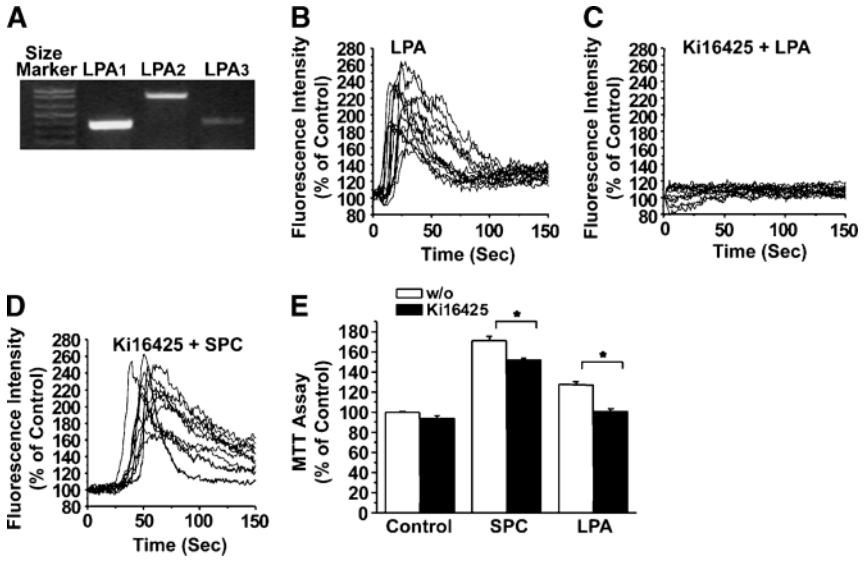

Fig. 7. Effects of Ki16425 on the SPC-induced increase of $[Ca^{2+}]_i$ and proliferation. A: The mRNA levels of lysophosphatidic acid (LPA) receptors (i.e., LPA_1, LPA_2, and LPA_3) in hADSCs were determined by RT-PCR analysis. B–D: Serum-starved hADSCs were loaded with fluo-4-AM for 40 min at 37°C in the absence or presence of 10 μM Ki16425 and then exposed to 5 μM LPA or 5 μM D-*erythro*-SPC as indicated. Ca^{2+}-dependent fluorescence was measured every second for the indicated times after the addition of LPA, and fluorescence intensities of >12 different cells from time-lapse images were quantified over time. Representative data from three similar experiments are shown. E: hADSCs were plated on 24-well culture plates, pretreated with 10 μM Ki16425 for 15 min, and then exposed to 5 μM D-*erythro*-SPC or 5 μM LPA for 48 h. Cell numbers were measured by the MTT assay, and results are shown as percentages of controls. Data are shown as means ± SEM ($n = 4$) and are representative of three independent experiments. * $P < 0.05$ by Student's *t*-test.

observed that PDGF as well as SPC stimulated the proliferation of hADSCs by a JNK-dependent pathway (48), and several recent studies demonstrated that the MEK-ERK-dependent pathway plays a key role in the induction of apoptosis (49–52). Therefore, these results support our conclusion that JNK, but not ERK, plays a crucial role in the SPC-induced proliferation of hADSCs.

By means of matrix-assisted laser desorption ionization time-of-flight mass spectrometry, the concentration of SPC was estimated at 50 nM in plasma and 130 nM in serum (53). We observed that proliferation of hADSCs was significantly increased in response to 50 nM SPC and dose-dependently stimulated, with a maximal increase at 5 μM SPC (Fig. 1A). It has been reported that SPC induces proliferation in the micromolar range up to 10 μM in several other cell types (15, 54). Because these concentration of SPC are higher than that found in plasma (53), the physiological relevance of the SPC-induced proliferation can

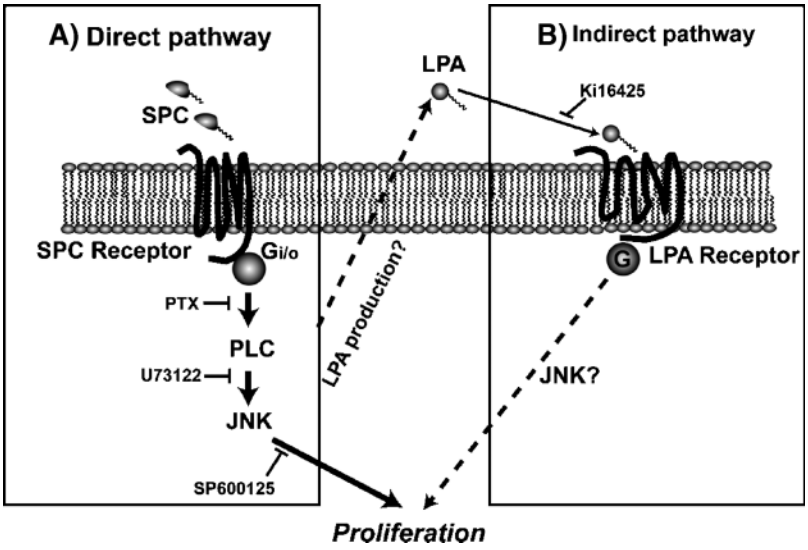

Fig. 8. Scheme of the molecular mechanisms involved in the SPC-induced proliferation of hADSCs. A: SPC treatment directly stimulates the proliferation of hADSCs through activation of the SPC receptor-Gi/Go-PLC-JNK pathway. B: SPC treatment causes production of LPA, and the subsequent LPA-induced activation of LPA receptors increases the proliferation of hADSCs.

be argued. SPC is unlikely to act as a hormone but rather as a paracrine mediator in local microenvironments. Furthermore, SPC is concentrated within lipoprotein particles, such as high density lipoproteins (55, 56). Therefore, the concentration of SPC in local microenvironments could not be clearly determined. Although the physiological relevance of SPC-induced proliferation has not been clarified, the stimulatory effect of SPC on the proliferation of hADSCs was almost comparable to that of PDGF-BB, which is a potent mitogen for mesenchymal cell types. This result raised the possibility that SPC may be useful for the in vitro amplification of hADSCs because of the immunogenic properties of FBS. However, the stimulatory effect of SPC on proliferation was not completely equivalent to the growth-promoting activity of 10% FBS. Therefore, combined treatment of SPC with other growth factors may be needed for the optimal amplification of hADSCs in vitro. The physiological significance of the SPC-induced proliferation of hADSCs within adipose tissues and the effects of SPC on the differentiation of hADSCs should be clarified further.

The authors thank Dr. Sung Ok Yoon (Ohio State University) for providing the adenoviruses bearing GFP plus DN-JNK2 or GFP. The authors also thank Dr. Young-Guen Kwon for providing the DN-MEK1 retroviral construct. This work was supported in part by the Korea Research Foundation (Grants KRF-2002-070-C00074 and KRF-2004-015-C00435).

REFERENCES

1. Barry, F. P., and J. M. Murphy. 2004. Mesenchymal stem cells: clinical applications and biological characterization. *Int. J. Biochem. Cell Biol.* **36:** 568–584.
2. Beresford, J. N., J. H. Bennett, C. Devlin, P. S. Leboy, and M. E. Owen. 1992. Evidence for an inverse relationship between the differentiation of adipocytic and osteogenic cells in rat marrow stromal cell cultures. *J. Cell Sci.* **102:** 341–351.
3. Prockop, D. J. 1997. Marrow stromal cells as stem cells for nonhematopoietic tissues. *Science.* **276:** 71–74.
4. Pittenger, M. F., A. M. Mackay, S. C. Beck, R. K. Jaiswal, R. Douglas, J. D. Mosca, M. A. Moorman, D. W. Simonetti, S. Craig, and D. R. Marshak. 1999. Multilineage potential of adult human mesenchymal stem cells. *Science.* **284:** 143–147.
5. Caplan, A. I. 1991. Mesenchymal stem cells. *J. Orthop. Res.* **9:** 641–650.
6. Short, B., N. Brouard, T. Occhiodoro-Scott, A. Ramakrishnan, and P. J. Simmons. 2003. Mesenchymal stem cells. *Arch. Med. Res.* **34:** 565–571.
7. Dart, A. M., and J. P. Chin-Dusting. 1999. Lipids and the endothelium. *Cardiovasc. Res.* **43:** 308–322.
8. Anliker, B., and J. Chun. 2004. Lysophospholipid G protein-coupled receptors. *J. Biol. Chem.* **279:** 20555–20558.
9. Meyer zu Heringdorf, D., H. M. Himmel, and K. H. Jakobs. 2002. Sphingosylphosphorylcholine—biological functions and mechanisms of action. *Biochim. Biophys. Acta.* **1582:** 178–189.
10. Spiegel, S., and S. Milstien. 2003. Sphingosine-1-phosphate: an enigmatic signalling lipid. *Nat. Rev. Mol. Cell Biol.* **4:** 397–407.
11. Boguslawski, G., D. Lyons, K. A. Harvey, A. T. Kovala, and D. English. 2000. Sphingosylphosphorylcholine induces endothelial cell migration and morphogenesis. *Biochem. Biophys. Res. Commun.* **272:** 603–609.
12. Desai, N. N., and S. Spiegel. 1991. Sphingosylphosphorylcholine is a remarkably potent mitogen for a variety of cell lines. *Biochem. Biophys. Res. Commun.* **181:** 361–366.
13. Xu, Y. 2002. Sphingosylphosphorylcholine and lysophosphatidylcholine: G protein-coupled receptors and receptor-mediated signal transduction. *Biochim. Biophys. Acta.* **1582:** 81–88.
14. Sun, L., L. Xu, F. A. Henry, S. Spiegel, and T. B. Nielsen. 1996. A new wound healing agent—sphingosylphosphorylcholine. *J. Invest. Dermatol.* **106:** 232–237.
15. Wakita, H., K. Matsushita, K. Nishimura, Y. Tokura, F. Furukawa, and M. Takigawa. 1998. Sphingosylphosphorylcholine stimulates proliferation and upregulates cell surface-associated plasminogen activator activity in cultured human keratinocytes. *J. Invest. Dermatol.* **110:** 253–258.
16. Chin, T. Y., and S. H. Chueh. 1998. Sphingosylphosphorylcholine stimulates mitogen-activated protein kinase via a Ca^{2+}-dependent pathway. *Am. J. Physiol.* **275:** C1255–C1263.
17. Yamada, T., F. Okajima, S. Ohwada, and Y. Kondo. 1997. Growth inhibition of human pancreatic cancer cells by sphingosylphosphorylcholine and influence of culture conditions. *Cell. Mol. Life Sci.* **53:** 435–441.
18. Jeon, E. S., Y. J. Kang, H. Y. Song, J. S. Woo, J. S. Jung, Y. K. Kim, and J. H. Kim. 2005. Role of MEK-ERK pathway in sphingosylphosphorylcholine-induced cell death in human adipose tissue-derived mesenchymal stem cells. *Biochim. Biophys. Acta.* **1734:** 25–33.
19. Chang, L., and M. Karin. 2001. Mammalian MAP kinase signalling cascades. *Nature.* **410:** 37–40.
20. Davis, R. J. 2000. Signal transduction by the JNK group of MAP kinases. *Cell.* **103:** 239–252.
21. Wada, T., and J. M. Penninger. 2004. Mitogen-activated protein kinases in apoptosis regulation. *Oncogene.* **23:** 2838–2849.
22. Seufferlein, T., and E. Rozengurt. 1995. Sphingosylphosphorylcholine activation of mitogen-activated protein kinase in Swiss 3T3 cells requires protein kinase C and a pertussis toxin-sensitive G protein. *J. Biol. Chem.* **270:** 24334–24342.
23. Sekiguchi, K., T. Yokoyama, M. Kurabayashi, F. Okajima, and R. Nagai. 1999. Sphingosylphosphorylcholine induces a hypertrophic growth response through the mitogen-activated protein kinase signaling cascade in rat neonatal cardiac myocytes. *Circ. Res.* **85:** 1000–1008.
24. Kang, S. K., D. H. Lee, Y. C. Bae, H. K. Kim, S. Y. Baik, and J. S. Jung. 2003. Improvement of neurological deficits by intracerebral transplantation of human adipose tissue-derived stromal cells after cerebral ischemia in rats. *Exp. Neurol.* **183:** 355–366.
25. Lee, R. H., B. Kim, I. Choi, H. Kim, H. S. Choi, K. Suh, Y. C. Bae, and J. S. Jung. 2004. Characterization and expression analysis of mesenchymal stem cells from human bone marrow and adipose tissue. *Cell. Physiol. Biochem.* **14:** 311–324.
26. Harrington, A. W., J. Y. Kim, and S. O. Yoon. 2002. Activation of Rac GTPase by p75 is necessary for c-jun N-terminal kinase-mediated apoptosis. *J. Neurosci.* **22:** 156–166.
27. Min, J. K., Y. M. Kim, Y. M. Kim, E. C. Kim, Y. S. Gho, I. J. Kang, S. Y. Lee, Y. Y. Kong, and Y. G. Kwon. 2003. Vascular endothelial growth factor up-regulates expression of receptor activator of NF-kappa B (RANK) in endothelial cells. Concomitant increase of angiogenic responses to RANK ligand. *J. Biol. Chem.* **278:** 39548–39557.
28. Moller, T., J. J. Contos, D. B. Musante, J. Chun, and B. R. Ransom. 2001. Expression and function of lysophosphatidic acid receptors in cultured rodent microglial cells. *J. Biol. Chem.* **276:** 25946–25952.
29. Fredriksson, L., H. Li, and U. Eriksson. 2004. The PDGF family: four gene products form five dimeric isoforms. *Cytokine Growth Factor Rev.* **15:** 197–204.
30. Meyer zu Heringdorf, D., N. Niederdraing, E. Neumann, R. Frode, H. Lass, C. J. Van Koppen, and K. H. Jakobs. 1998. Discrimination between plasma membrane and intracellular target sites of sphingosylphosphorylcholine. *Eur. J. Pharmacol.* **354:** 113–122.
31. Hazzalin, C. A., E. Cano, A. Cuenda, M. J. Barratt, P. Cohen, and L. C. Mahadevan. 1996. p38/RK is essential for stress-induced nuclear responses: JNK/SAPKs and c-Jun/ATF-2 phosphorylation are insufficient. *Curr. Biol.* **6:** 1028–1031.
32. Malchinkhuu, E., K. Sato, Y. Horiuchi, C. Mogi, S. Ohwada, S. Ishiuchi, N. Saito, H. Kurose, H. Tomura, and F. Okajima. 2005. Role of p38 mitogen-activated kinase and c-Jun terminal kinase in migration response to lysophosphatidic acid and sphingosine-1-phosphate in glioma cells. *Oncogene.* **24:** 6676–6688.
33. Marinissen, M. J., and J. S. Gutkind. 2001. G-protein-coupled receptors and signaling networks: emerging paradigms. *Trends Pharmacol. Sci.* **22:** 368–376.
34. Ye, X., I. Ishii, M. A. Kingsbury, and J. Chun. 2002. Lysophosphatidic acid as a novel cell survival/apoptotic factor. *Biochim. Biophys. Acta.* **1585:** 108–113.

35. Siehler, S., and D. R. Manning. 2002. Pathways of transduction engaged by sphingosine 1-phosphate through G protein-coupled receptors. *Biochim. Biophys. Acta.* **1582:** 94–99.
36. Gutkind, J. S. 2000. Regulation of mitogen-activated protein kinase signaling networks by G protein-coupled receptors. *Sci. STKE.* **40:** RE1.
37. Yamauchi, J., T. Kawano, M. Nagao, Y. Kaziro, and H. Itoh. 2000. G(i)-dependent activation of c-Jun N-terminal kinase in human embryonal kidney 293 cells. *J. Biol. Chem.* **275:** 7633–7640.
38. Murakami, N., T. Yokomizo, T. Okuno, and T. Shimizu. 2004. G2A is a proton-sensing G-protein coupled receptor antagonized by lysophosphatidylcholine. *J. Biol. Chem.* **279:** 42484–42491.
39. Bektas, M., L. S. Barak, P. S. Jolly, H. Liu, K. R. Lynch, E. Lacana, K. B. Suhr, S. Milstien, and S. Spiegel. 2003. The G protein-coupled receptor GPR4 suppresses ERK activation in a ligand-independent manner. *Biochemistry.* **42:** 12181–12191.
40. Ludwig, M. G., M. Vanek, D. Guerini, J. A. Gasser, C. E. Jones, U. Junker, H. Hofstetter, R. M. Wolf, and K. Seuwen. 2003. Proton-sensing G-protein-coupled receptors. *Nature.* **425:** 93–98.
41. Xie, Y., and K. E. Meier. 2004. Lysophospholipase D and its role in LPA production. *Cell. Signal.* **16:** 975–981.
42. Moolenaar, W. H., L. A. van Meeteren, and B. N. Giepmans. 2004. The ins and outs of lysophosphatidic acid signaling. *Bioessays.* **26:** 870–881.
43. Manning, A. M., and R. J. Davis. 2003. Targeting JNK for therapeutic benefit: from junk to gold? *Nat. Rev. Drug Discov.* **2:** 554–565.
44. Du, L., C. S. Lyle, T. B. Obey, W. A. Gaarde, J. A. Muir, B. L. Bennett, and T. C. Chambers. 2004. Inhibition of cell proliferation and cell cycle progression by specific inhibition of basal JNK activity: evidence that mitotic Bcl-2 phosphorylation is JNK-independent. *J. Biol. Chem.* **279:** 11957–11966.
45. Schwabe, R. F., C. A. Bradham, T. Uehara, E. Hatano, B. L. Bennett, R. Schoonhoven, and D. A. Brenner. 2003. c-Jun-N-terminal kinase drives cyclin D1 expression and proliferation during liver regeneration. *Hepatology.* **37:** 824–832.
46. Zhan, Y., S. Kim, Y. Izumi, Y. Izumiya, T. Nakao, H. Miyazaki, and H. Iwao. 2003. Role of JNK, p38, and ERK in platelet-derived growth factor-induced vascular proliferation, migration, and gene expression. *Arterioscler. Thromb. Vasc. Biol.* **23:** 795–801.
47. Kavurma, M. M., and L. M. Khachigian. 2003. ERK, JNK, and p38 MAP kinases differentially regulate proliferation and migration of phenotypically distinct smooth muscle cell subtypes. *J. Cell. Biochem.* **89:** 289–300.
48. Kang, Y. J., E. S. Jeon, H. Y. Song, J. S. Woo, J. S. Jung, Y. K. Kim, and J. H. Kim. 2005. Role of c-Jun N-terminal kinase in the PDGF-induced proliferation and migration of human adipose tissue-derived mesenchymal stem cells. *J. Cell Biochem.* **95:** 1135–1145.
49. Lieu, C. H., C. C. Liu, T. H. Yu, K. D. Chen, Y. N. Chang, and Y. K. Lai. 1998. Role of mitogen-activated protein kinase in taxol-induced apoptosis in human leukemic U937 cells. *Cell Growth Differ.* **9:** 767–776.
50. Nguyen, T. T., E. Tran, T. H. Nguyen, P. T. Do, T. H. Huynh, and H. Huynh. 2004. The role of activated MEK-ERK pathway in quercetin-induced growth inhibition and apoptosis in A549 lung cancer cells. *Carcinogenesis.* **25:** 647–659.
51. Kalechman, Y., D. L. Longo, R. Catane, A. Shani, M. Albeck, and B. Sredni. 2000. Synergistic anti-tumoral effect of paclitaxel (Taxol)+AS101 in a murine model of B16 melanoma: association with ras-dependent signal-transduction pathways. *Int. J. Cancer.* **86:** 281–288.
52. Kim, G. S., J. S. Hong, S. W. Kim, J. M. Koh, C. S. An, J. Y. Choi, and S. L. Cheng. 2003. Leptin induces apoptosis via ERK/cPLA2/cytochrome c pathway in human bone marrow stromal cells. *J. Biol. Chem.* **278:** 21920–21929.
53. Liliom, K., G. Sun, M. Bunemann, T. Virag, N. Nusser, D. L. Baker, D. A. Wang, M. J. Fabian, B. Brandts, K. Bender, et al. 2001. Sphingosylphosphocholine is a naturally occurring lipid mediator in blood plasma: a possible role in regulating cardiac function via sphingolipid receptors. *Biochem. J.* **355:** 189–197.
54. Desai, N. N., R. O. Carlson, M. E. Mattie, A. Olivera, N. E. Buckley, T. Seki, G. Brooker, and S. Spiegel. 1993. Signaling pathways for sphingosylphosphorylcholine-mediated mitogenesis in Swiss 3T3 fibroblasts. *J. Cell Biol.* **121:** 1385–1395.
55. Nofer, J. R., B. Levkau, I. Wolinska, R. Junker, M. Fobker, A. von Eckardstein, U. Seedorf, and G. Assmann. 2001. Suppression of endothelial cell apoptosis by high density lipoproteins (HDL) and HDL-associated lysosphingolipids. *J. Biol. Chem.* **276:** 34480–34485.
56. Sachinidis, A., R. Kettenhofen, S. Seewald, I. Gouni-Berthold, U. Schmitz, C. Seul, Y. Ko, and H. Vetter. 1999. Evidence that lipoproteins are carriers of bioactive factors. *Arterioscler. Thromb. Vasc. Biol.* **19:** 2412–2421.